J Mater Sci (2009) 44:2206–2217
DOI 10.1007/s10853-008-3196-7

FESTSCHRIFT IN HONOUR OF PROF T R ANANTHARAMAN ON THE OCCASION OF HIS 80TH BIRTHDAY

Phase field modeling of grain growth: effect of boundary thickness, triple junctions, misorientation, and anisotropy

I. M. McKenna · M. P. Gururajan · P. W. Voorhees

Received: 28 May 2008 / Accepted: 15 December 2008 / Published online: 22 January 2009

Abstract Phase-field models based on multiple order parameters are used extensively to study grain growth in polycrystalline materials. However, if simulations are to be carried out using experimentally obtained microstructures as the initial condition, and the resultant microstructures are to be carefully compared with those obtained from experiments, then the parameters used in the numerical simulations need to be benchmarked with analytical solutions. Furthermore, the models themselves need to be modified to incorporate the dependence of grain boundary energy on misorientation across the boundary as well as the anisotropy in the boundary energy for any given misorientation that stems from the planes of different grains that make up the boundary. In this article, we address both these issues and present some preliminary results from our 2D and 3D simulations.

Introduction

Discovered in the mid-eighteenth century, grain boundaries are probably the longest known crystalline defects [1]. They play a key role in determining the structure and properties of metals, alloys, semiconductors, and ceramics, which are some of the materials of industrial importance [1–5]. Further, the structure and properties of grain boundaries are also of interest by themselves from the point of view of a fundamental understanding of materials and their microstructure [6]. Hence, grain boundaries are being extensively studied using experiments, models, and numerical simulations. These studies are far too varied, detailed, and numerous to be summarized here; see the excellent monographs of Sutton and Balluffi [2], Gottstein and Shvindlerman [1], Humphreys and Heatherly [3], and so on.

It is well known that in polycrystalline samples held at high enough temperatures the microstructure evolves in such a way that the overall average grain size increases while the number of grains in the system decreases. This process is known as grain growth, and is driven by the energy and curvature of the grain boundary (GB). In particular, in 2D, assuming (a) isotropic GB energies and (b) local equilibrium at triple junctions, the rate of growth of a grain can be shown to be purely driven by its topology, namely, the number of its sides [7, 8]; in 3D, under the same assumptions, the growth rate is no longer purely topological but is more involved [9].

Grain growth in a generic microstructure typically involves events such as the disappearance of grains, merging of boundaries, face switching events, and other such topological singularities. Hence, among the numerical studies, phase field models, which are ideal for simulations at mesoscopic length scales [10] and do not explicitly track the interface (and therefore naturally account for the topological singularities), are ideally suited for the study of grain growth and have been used extensively in the past decade; see the review by Chen [11]. A majority of these phase field models also assume isotropic interfacial energies. However, in most materials of industrial importance, the GB energies depend both on the misorientation across the boundary and the planes of the grains that make up the boundary (anisotropy). Therefore, we wish to modify the

I. M. McKenna (✉) · M. P. Gururajan · P. W. Voorhees
Department of Materials Science and Engineering, Northwestern University, Evanston, IL 60208, USA
e-mail: i-mckenna@northwestern.edu

Present Address:
M. P. Gururajan
Department of Applied Mechanics, Indian Institute of Technology – Delhi, Hauz Khas, New Delhi 110016, India

existing phase field models to incorporate the misorientation and anisotropy dependence of GB energy. Along the way, we also wish to benchmark the existing phase field models by comparing the results obtained from them using model systems with the analytical results in order to identify the range of parameters for the phase field for which the results are reliable.

In this article, in the following section we describe (albeit very briefly) our modified phase field model; the details can be found elsewhere [12]. Then, in sections "Effect of boundary thickness" and "Effect of triple point junctions coupled with boundary thickness," we present some of the benchmark studies that we have carried out in 2D, which indicate the effect of boundary thickness and triple junctions on grain growth. These benchmark studies also give us a couple of rules of thumb to be aware of while using experimentally measured grain structures in simulations, or while comparing the numerical results with experimental ones. Finally, in section "Effect of misorientation/anisotropy on kinetics and morphology," we examine the effect of misorientation on GB energy in 1D and report some of the preliminary results on both 2D and 3D systems which clearly demonstrate the effects of anisotropy and misorientation on grain growth, and the article is ended with a brief summary.

Formulation

In phase field models the microstructure is described using field variables known as order parameters. In particular, for describing a polycrystalline microstructure a multi-order parameter model is used; where for each distinct grain orientation, p, a corresponding order parameter η_p is assigned. Thus, if there are N distinct orientations in a given system a total number of N-order parameters are needed; these N-order parameters can be ordered to form an N-vector field. The order parameters are continuous functions bounded between zero and unity. For any given grain with an orientation, M, the Mth component of the N-vector is unity and all the other components are zero. In those regions where grains with different orientations meet, more than one component of the N-vector take on values between zero and unity; for example, at a GB there are two non-zero components, three at triple point junctions, four at quadruple point junctions, and so on.

Given such a description of the polycrystalline microstructure, the free energy is typically written as a function of the order parameters and their gradients, assuming (a) that the GB energies are independent of the misorientation across the boundary, and (b) that the GB energy is isotropic [13, 14]. However, in this article, we report the results obtained using a modified model in which the GB energy is anisotropic and is dependent on the misorientation. The misorientation dependence is incorporated by making the gradient energy coefficient dependent on the order parameters and orientation of the grains. The anisotropy is incorporated using higher-order gradients and their associated tensor gradient energy coefficients in the free energy functional.

The fourth-rank tensor gradient energy coefficients that are used are the same as those used (in the context of precipitation) by Abinandanan and Haider [15]. However, in this implementation, the tensor terms must also be transformed to the computational frame of reference since we are dealing with grains of differing orientations. The coordinate transformations on the tensor coefficients, as well as the calculation of misorientation that is consistent with the underlying cubic symmetry of the crystallites, are achieved using quaternions which are associated with each orientation, and hence with each order parameter. The details of the algebra involving the quaternions are reported elsewhere [12]. The modifications in our model system are from two differences. The first coming from the addition of an anisotropy term, f_a, in the free energy, and the other from taking the constant gradient energy coefficient, κ_p, and allowing it to be a function of both the misorientation and nonzero-order parameters at each respective grid position.

We take the free energy, F, to be:

$$F = \int_V [f_b + f_m + f_a] dV, \tag{1}$$

where V is the volume of the system, f_b the bulk-free energy density, f_m the energy due to the misorientation between grains, and f_a is the energy that will change with the orientation of the GB plane.

The bulk-free energy is given by the following expression [13]:

$$f_b(\eta_1, \eta_2, \ldots, \eta_p, \ldots, \eta_N) = \mu\left(\sum_{i=1}^{N}\left(-\frac{a}{2}\eta_i^2 + \frac{b}{4}\eta_i^4\right) + c\sum_{i=1}^{N}\sum_{j\neq i}^{N}\eta_i^2\eta_j^2\right), \tag{2}$$

where μ, a, b, and c are constants. The constraint $c > b/2$ should be satisfied to make sure that there are N degenerate minima associated with the N unit vectors located at: $(\eta_1, \eta_2, \ldots, \eta_N) = (1, 0, \ldots, 0), \ldots, (0, 0, \ldots, 1)$ [16]. The constant μ is used to adjust the interface thickness by modifying the height of the energy barrier between the minima such that the thickness of the boundary is proportional to the magnitude of μ [17].

The misorientation energy is given by:

$$f_m = \sum_{p=1}^{N} \kappa_p |\nabla \eta_p|^2, \tag{3}$$

where κ_p is the scalar gradient energy coefficient which is both a function of the order parameters and the grain

orientations. For a certain model of the GB energy on misorientation κ_p can be expressed as:

$$\kappa_p = \kappa_0 + \sum_{q\neq p, q=1}^{N} \eta_q |\theta_{pq}|, \tag{4}$$

where κ_0 is a constant and θ_{pq}, in radians, is the misorientation across the GB corresponding to two grains with order parameters p and q. For this particular model, the GB energy scales linearly with misorientation, but can be modified to capture Read-Shockley type behavior [15].

The anisotropic energy is given by the following expression:

$$\begin{aligned} f_a = \sum_{p=1}^{N} \Bigg(& \alpha^p_{ijkl} \left(\frac{\partial \eta_p}{\partial x_i}\right)\left(\frac{\partial \eta_p}{\partial x_j}\right)\left(\frac{\partial \eta_p}{\partial x_k}\right)\left(\frac{\partial \eta_p}{\partial x_l}\right) \\ & + \beta^p_{ijkl} \left(\frac{\partial^2 \eta_p}{\partial x_i \partial x_j}\right)\left(\frac{\partial \eta_p}{\partial x_k}\right)\left(\frac{\partial \eta_p}{\partial x_l}\right) \\ & + \gamma^p_{ijkl} \left(\frac{\partial^2 \eta_p}{\partial x_i \partial x_j}\right)\left(\frac{\partial^2 \eta_p}{\partial x_k \partial x_l}\right) \Bigg), \end{aligned} \tag{5}$$

where α^p_{ijkl}, β^p_{ijkl}, and γ^p_{ijkl} are the tensor coefficients, and are identical to those used by Abinandanan and Haider [15], but rotated to the computational frame of reference from the principle coordinate system of the pth grain. By assuming cubic anisotropy γ^p_{ijkl} involves only three independent coefficients, two of which are always found in linear combination. Therefore the tensor can be completely defined with two parameters, which we introduce as γ_{aniso} and γ_{iso} for the tensor γ^p_{ijkl}. They are defined in the principle coordinate frame of reference (which is equivalent in both 2D and 3D) as:

$$\gamma_{\text{aniso}} = \gamma_{1111} - \gamma_{1122} - 2\gamma_{1212}, \tag{6}$$

$$\gamma_{\text{iso}} = \gamma_{1122} + 2\gamma_{1212}, \tag{7}$$

where γ_{aniso} is the term which specifies the amount of anisotropy in the system and γ_{iso} is a term chosen to insure that the system is stable against large wave number fluctuations [5].

Given the free energy the order parameters are evolved using the Allen–Cahn (or time dependent Ginsburg-Landau) equation. This is because the order parameters corresponding to the grain orientations are non-conserved quantities. Thus, the spatiotemporal evolution is given by

$$\frac{\partial \eta_p}{\partial t} = -L_p \left(\frac{\delta F}{\delta \eta_p}\right), \quad (p = 1, \ldots N), \tag{8}$$

where L_p is the kinetic coefficient corresponding to the order parameter η_p, and $\delta/\delta\eta_p$ is the variational derivative with respect to η_p. The detailed expressions for the variational derivatives are straightforward to obtain, and are reported elsewhere [12].

Numerical implementation

In all the simulations reported in this article, for the sake of simplicity, the tensor coefficients α^p_{ijkl} and β^p_{ijkl} are assumed to be identically zero. Furthermore, for the 2D simulations reported in sections "Effect of boundary thickness" and "Effect of triple point junctions coupled with boundary thickness," we also assume that the gradient energy coefficient, κ_p, is a constant and the fourth-rank tensor coefficients, γ^p_{ijkl}, are identically zero. In other words, the GB energy is isotropic and is independent of the order parameters and the orientations of the grains. The explicit Forward Euler finite differencing scheme (for the 2D simulations), and semi-implicit Fourier spectral method (for the 3D simulations) are used to integrate Eq. 8. The two different methods are used in order to show that the model is applicable to a variety of different techniques as well as a manner in which to check between the two different implementations. For the finite difference scheme, the Laplacian is solved using a second-order accurate central second differencing formula; the details and stencils used for the anisotropy and misorientation are discussed elsewhere [18]. Furthermore, the details of the semi-implicit Fourier spectral implementation can be found in reference [12]. All simulations are carried out assuming periodic boundary conditions.

For multi-order parameter models of the type described above, when the system dimensions, size, and the number of distinct grain orientations are large, the numerical simulations can both be processor and memory intensive. Usually, in such cases, a sparse matrix algorithm becomes necessary and is implemented [18–22]. However, for the results reported in this article such algorithms are unnecessary.

Results and discussion

In this section, a brief description of the analytical sharp-interface result for growth rates of grains with isotropic boundary energy in 2D is revisited. Next, we report the results from our 2D studies on the effect of the boundary thickness and triple junctions on grain growth. These results are then used to benchmark and identify parameter regimes in which the results from the phase field model deviates from those obtained using the sharp interface models. Next we use these results to make sure our interfaces are properly resolved in the investigation of adding misorientation and anisotropy into the system. With the modified phase field model we then study the effects of varying the misorientation between grains as well as the parameters γ_{aniso} and γ_{iso} which are used to modify the anisotropy of the system. Finally, we present some

preliminary results on 3D systems that show the importance of both misorientation and anisotropy on the resulting grain shapes and that the model is easily extendable to 3D.

2D von Neumann–Mullins relation

In the following section, we present results from our 2D simulation and compare them with the corresponding analytical ones. Hence, before presenting the numerical results, we wish to summarize the analytical results on grain growth in 2D, specifically for systems with isotropic boundary energy (with and without triple point junctions).

In 2D, the kinetics of grain growth in systems with isotropic boundary energy is solely determined by the topology of the grains. This result, known as the von Neumann–Mullins relation, is obtained by using the well-known fact that GB motion is driven by the mean curvature. Explicitly, the boundary moves with a velocity, v, which is proportional to the mean curvature:

$$v = -L\sigma H, \tag{9}$$

where L is the (constant) isotropic boundary mobility, σ the (constant) isotropic boundary energy, and H is the mean curvature of the boundary. The minus sign indicates that the interface moves toward its center of curvature. Using this relation, the local expression for the change in area, A, of a grain can be calculated by integrating the velocity along the GB:

$$\frac{\mathrm{d}A}{\mathrm{d}t} = \oint_{\mathrm{GB}} v\mathrm{d}l = -\oint_{\mathrm{GB}} L\sigma H\mathrm{d}l. \tag{10}$$

The mean curvature, H, of the boundary is related to the tangent angle, ψ, of the boundary and the boundary element, l, as follows: $H = \mathrm{d}\psi/\mathrm{d}l$ [1]. Hence,

$$\frac{\mathrm{d}A}{\mathrm{d}t} = -L\sigma \oint_{\mathrm{GB}} \frac{\mathrm{d}\psi}{\mathrm{d}l}\mathrm{d}l = -L\sigma \int_0^{2\pi} \mathrm{d}\psi. \tag{11}$$

For an enclosed continuous surface the line integral would be 2π. However, since there are discontinuities around the triple points, with a turning angle equal to $\xi_i = \pi/3$ for a system with isotropic boundary energies, this value must be subtracted from 2π for each triple point junction present. A schematic of this discontinuous change in curvature around the triple point junctions for an isolated grain is shown in Fig. 1. Hence, evaluating the integral in Eq. 11 we obtain

$$\frac{\mathrm{d}A}{\mathrm{d}t} = -L\sigma\left(2\pi - \sum_{i=1}^{n}\xi_i\right) = -L\sigma\left(2\pi - \frac{n\pi}{3}\right) = \frac{L\sigma\pi}{3}(n-6). \tag{12}$$

Thus, from the expression above, it is clear that one need only know the number of triple points, or equivalently

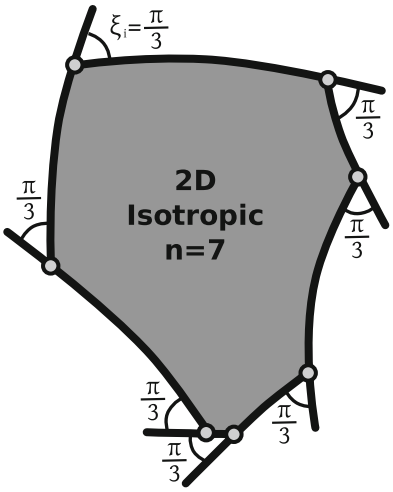

Fig. 1 A example schematic of a seven-sided grain in an isotropic system where the turning angles around the triple points are equivalent and equal to $\pi/3$

sides of a grain, to calculate the rate of area change of that grain and this rate is independent of its corresponding area or perimeter. Secondly, it shows that the area of a grain scales linearly with time. It is also obvious that a grain with $n = 6$ sides does not grow or shrink, while ones with more than six sides grow and those with less than six sides shrink.

Effect of boundary thickness

In the following simulations, we have used $a = b = c = L_p = \kappa_p = 1$ and $\Delta t = 0.01$ for the cases where $\Delta x = \Delta y = 0.5$ or $\Delta x = \Delta y = 1$. In cases where the interface is very sharp, a finer spatial discretization is necessary ($\Delta x = \Delta y < 0.5$ and hence a Δt smaller than 0.01) to make sure that there are enough points through the interface and to avoid numerical artifacts such as grid-imposed anisotropy.

In this section we investigate the effects of interface thickness on the shrinkage kinetics of a small grain by comparing the phase field results with those given by the von Neumann–Mullins expression [23]. To accomplish this task, $\mathrm{d}A/\mathrm{d}t$ was measured throughout the entire simulation and plotted against the radius normalized by the interface thickness. The rate of area change is then normalized by the growth rate obtained from the von Neumann–Mullins equation, Eq. 12 (denoted as $\mathrm{d}A^*/\mathrm{d}t$). This is easily done since the number of sides of the grain simulated is constant throughout the evolution. In cases where the grain shape is not circular, an effective grain radius given by $\sqrt{A/\pi}$ is used. A second series of tests conducted measured the velocity and curvature of the interface and compared this to theoretical values as a function of the radius normalized by interface thickness. This allows for a comparison of

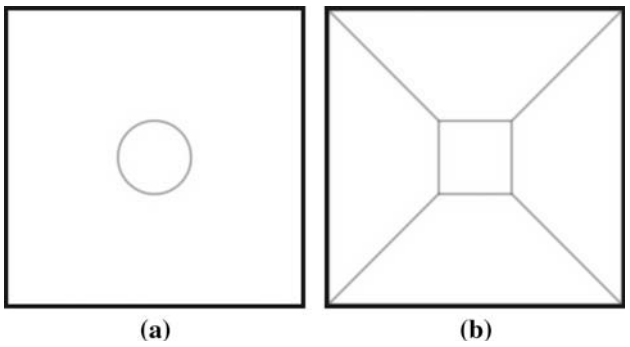

Fig. 2 Initial conditions for **a** two-grain and **b** five-grain geometries in 2D

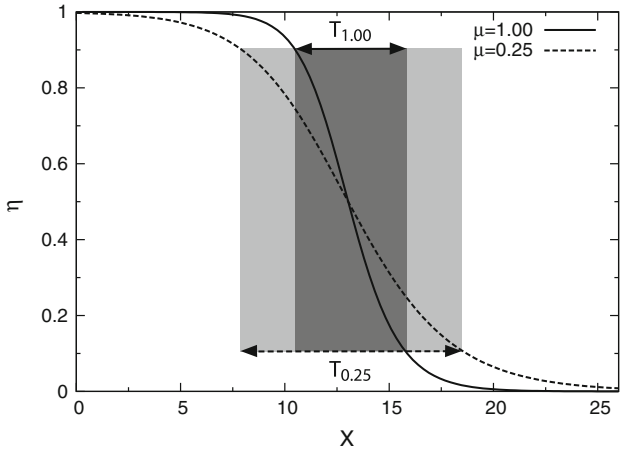

Fig. 3 Interface thickness, T, as a function of position for two values of μ

deviation between theory and simulation between the two methods as well as further understanding into the effect of triple point junctions on the shrinkage rate of a grain using a phase field simulation.

In Fig. 2, we show the initial conditions used for the two- and five-grain systems on a 1024 × 1024 simulation cell (for a value of $\mu = 0.1$); these figures are the summation of the square of the order parameters and the non-white regions correspond to the grain boundaries while the bulk of the grains is shown in white. Since (for the grains at the center of the simulation cell) there are no triple junctions in the two-grain case, and four in the five-grain case, the growth rates for the two cases are given by the corresponding von Neumann–Mullins expressions:

$$\frac{dA}{dt} = \frac{(1)(2)\pi}{3}(4-6) \approx -4.19; \tag{13}$$

$$\frac{dA}{dt} = \frac{(1)(2)\pi}{3}(0-6) \approx -12.57. \tag{14}$$

The phase field models we are using are basically Allen–Cahn equations that describe the motion of antiphase domain boundaries. Allen and Cahn [24] showed that in this case the velocity of the boundary is independent of the boundary energy and dependent only on the product of the interfacial mobility and the gradient energy coefficient. Thus the velocity of the grain should be independent of μ, since μ only varies the thickness of the boundary. The mean curvature, H, of the grains and the velocity of the boundary are calculated numerically at the centers of the sides of the grain, with normals pointing away from the centers of the simulation cells. The mean curvature is calculated and then interpolated to the point at which $\eta = 0.5$. The velocity of the interface is calculated by tracking the evolution of the $\eta = 0.5$ level curve through a cubic spline interpolation [25]. Note that $R = 1/H$ holds only for the two-grain case where the central grain is circular. Finally, the interface thickness was calculated along the $\langle 10 \rangle$ direction, which is normal to the interface, and is the distance over which the order parameter changes from 0.10 to 0.90. This is shown schematically in Fig. 3 by plotting the variation of two-order parameters through the interface for two different values of μ and determining the thicknesses, T.

The interface thickness, T, is useful for calculating the grid spacing necessary to obtain a specific number of points through the interface, I_{pts}. For example using a grid spacing of $\Delta x = \Delta y = 1$ with $\mu = 0.25$ yields $I_{\text{pts}} = 11$. When comparing this to the analytical result given by Moelans et al. [6], albeit with a different method used to calculate the interfacial thickness, the results presented here for the dependence of thickness on μ are in good agreement. By assuming the thickness calculated by the different methods in the two papers are linearly related the thickness presented here is a factor of 1.35 times thicker than in the article by Moelans et al. [6]. This comparison is possible because they use the same bulk-free energy to within a constant of the bulk-free energy used here. Using this result in their analytical expression and accounting for the different definitions of the gradient energy coefficient gives the following:

$$T = 1.348\sqrt{\frac{(8)(2)\kappa_p}{\mu}} = \frac{5.39}{\sqrt{\mu}}. \tag{15}$$

The factor of 1.35 was numerically calculated from the measurements of the interface thickness in 2D simulations, but Eq. 15 can also be analytically computed in 1D. Both 1D analytical and 2D simulation methods yield nearly identical equations for the thickness. Therefore the dependence of the thickness on interfacial curvature is small.

Since the grains grow according to Eq. 9, the GB velocity is proportional to the GB energy so we take $\sigma = 2\kappa_p$ [24, 26]. In Fig. 4, we show the boundary velocity divided by the mean curvature and normalized by $-L\sigma$

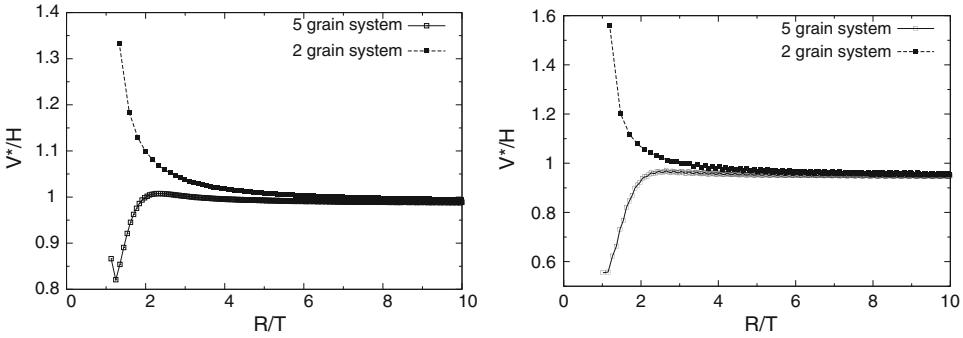

Fig. 4 Velocity divided by grain boundary curvature along $\langle 10 \rangle$, normalized by $-L\sigma$, plotted against the radius of the grain, normalized by the thickness of the interface, for two-grain and five-grain systems where **a** $I_{pts} = 11$ and **b** $I_{pts} = 6$

(denoted as V^*/H) as a function of R/T. It is clear that for large grain sizes the velocity divided by the mean curvature is indeed a constant and is equal to $-L\sigma = -L(2\kappa_p) = -2$, since $\kappa_p = 1$ in the calculations. When comparing this result to the phase field simulations as shown in Fig. 4 we see that the simulation and sharp interface results are in good agreement for $R/T > 6$ where $I_{pts} = 11$. When $R \gg T$ there is 1 and 5% error for when $I_{pts} = 11$ and $I_{pts} = 6$, respectively. One interesting result to note is that for small grain sizes the five-grain system curve deviates downward from the analytical result, whereas the two-grain system curve deviates upward. In the two-grain case it appears that the velocity of the interface increases faster than the analytical result since the geometry of the grain and thus curvature of the interface is completely defined for a specific radius of the grain. In order to help explain what is occurring in the five-grain case, when $R/T < 6$, we examine the velocity and curvature of the interface. The velocity is relatively constant until $R/T < 4$ where the velocity begins to increase steadily. This is also true of the curvature, H, where the rate of curvature change begins to sharply accelerate when $R/T < 4$. As $R/T \rightarrow 0$ the curvature increases faster than the velocity of the interface. This is a result of the triple point junctions moving faster than the sharp interface theory predicts.

In Fig. 5, the normalized rate of change of area, dA^*/dt, is plotted for the two- and five-grain systems for varying values of I_{pts}. When $I_{pts} \geq 11$ the curves overlap showing that there is nearly no effect of increasing the number of points through the interface beyond 11. A second point to note is that as R/T increases the results converge to the sharp interface limit. When $R \gg T$ the error associated with $I_{pts} = 4$, $I_{pts} = 6$, $I_{pts} = 11$ for the two-grain system is 3.5, 1.4, 0.4%, respectively. For the five-grain system using the same number of interface points there is 5.0, 1.9, 1.0% error. Thus the presence of triple point junctions appears to increase the error slightly when comparing it to a system with the same number of interface points and no triple point junctions. These errors are similiar to those reported in the previous papers [6, 17, 26]. The presence of these errors results in shifting the V^*/H and dA^*/dt asymptotic values toward lower values (corresponding to a more positive un-normalized shrinkage rate) than what the theory predicts and as a result has been shown to slow the shrinkage rate of the grains in this study. Furthermore, when $R/T \rightarrow 0$ the kinetics deviate from the von Neumann–Mullins sharp interface limit. Thus, using Fig. 5 it is possible to choose the thickness of the interface needed to yield an accurate value of the interface velocity as given in the phase field model.

Consistent with the predictions of sharp interface theory of the Allen–Cahn equations employed in these simulations we find that the interface parameter, μ, can be modified without it affecting the kinetics of boundary motion.

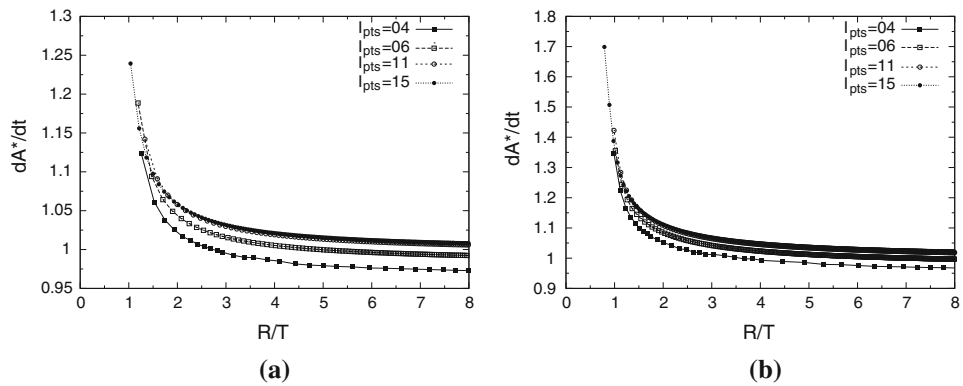

Fig. 5 dA/dt normalized by the predictions of von Neumann–Mullins for **a** two-grain and **b** five-grain system for varying number of interfacial points

Therefore one is free to use either μ, the grid spacing, or a combination of the two in order to change the number of points through the interface independent of the resulting output. This is why I_{pts} is used in Fig. 5. To be sure that one is examining only the influence of the thickness of the boundary on the interface evolution kinetics a sufficient number of points through the interface must be present in order to accurately represent the order parameter profile through the interface. In this study, it was found that $I_{pts} \geq 11$ yields converged solutions, however, employing $I_{pts} = 6$ yields reasonable values that, depending upon the application, may be acceptable.

Effect of triple point junctions coupled with boundary thickness

Moelans et al. [6] finds that R/T should be greater than 3 to be in the converged limit, where T is defined by Eq. 15. However, to calculate the minimum value of R/T required for convergence we examined both system geometries, as shown in Fig. 6, and used the system with largest deviation from theory. Then allowing for a tolerance of up to 10% error in the deviation from von Neumann–Mullins law using Fig. 5, we find that R/T should be greater than 2 to be in the converged limit, which is very close to that found by Moelans et al. [6]. One can use a more or less stringent criteria for convergence depending upon the degree of precision required for a calculation, but for the context of this paper $R/T < 2$ is defined to be in the unconverged limit. With this definition one can then calculate a rough estimate for the discretization of the simulation domain necessary to achieve a desired accuracy while using experimental data in the simulations. Assuming that all grains are approximately square-like and that they tessellate the given area, a simple calculation yields an estimate of the maximum number of grains in a converged system. For a 1024×1024 domain with $I_{pts} = 11$, and using a R/T cutoff value of 2, a maximum of 541 grains can be employed in the phase field calculation. However, as grains coarsen, if there are a large number of grains that are near the cutoff value then as the system continues to evolve the kinetics could substantially deviate as more grains shrink below the threshold value. Therefore the grain size distribution should also be such that the average-sized grain is sufficiently larger than the cutoff value for converged calculations to insure that a significant number of small grains satisfy the criterion. Depending upon the tolerable error it may then become necessary to parallelize systems among multiple processors or implement some type of algorithm to reduce processor workloads and memory resources [18–22].

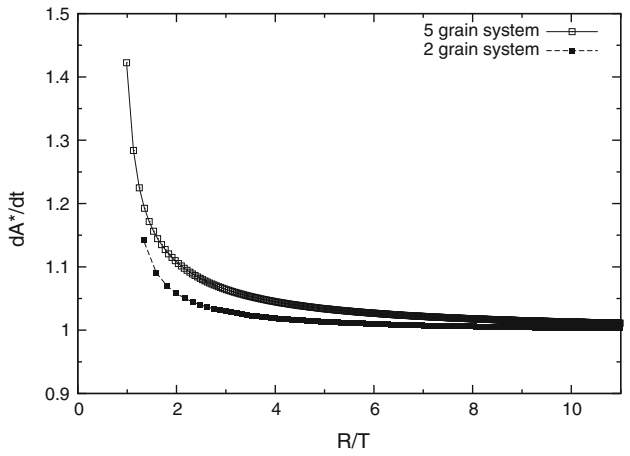

Fig. 6 dA/dt normalized by von Neumann–Mullins for 1024×1024 two-grain and five-grain systems where $I_{pts} = 11$

Examining the five- and two-grain systems, we can also identify the effect triple point junctions have on ideal kinetics of grain boundary motion in the phase field method. Since the triple junction is not sharp in the phase field model, its diffuseness could, in principal, affect the motion of the boundaries. From Fig. 6, it is clear that the presence of triple point junctions increases the R/T value at which the numerical results converge with theory. In cases where the boundaries are sufficiently thin relative to the size of the grain, so that agreement with von Neumann–Mullins is obtained, no triple point junction drag is observable. However, in the unconverged limit, when $R/T < 2$, the presence of triple point junctions actually increases the grain shrinkage rate. Furthermore, when considering Figs. 4 and 6, both indicate that the accelerated shrinkage rate of small four-sided grains supports the observation that triple junctions enhance the shrinkage rate of small grains.

Effect of misorientation/anisotropy on kinetics and morphology

In this section, we benchmark on the accuracy of the misorientation in 1D as a function of points through the interface. We continue to benchmark the modified model, by varying misorientation and anisotropy parameter values, in 2D. Finally, we present some preliminary results from our simulations on 3D systems in which the GB energy is dependent both on the misorientation and the anisotropy.

For all the results below the modified model for misorientation and anisotropy was used with a value of $\Delta x = \Delta y = \kappa_0 = 1$ and $\gamma_{iso} = -5$ and $\gamma_{aniso} = 15$ except when explicitly stated otherwise. Unlike the previous isotropic case, the thickness of the interface can now vary with misorientation between grains and the direction of the normal taken along the interface due to the underlying anisotropy. We report the values of I_{pts} along the $\langle 10 \rangle$

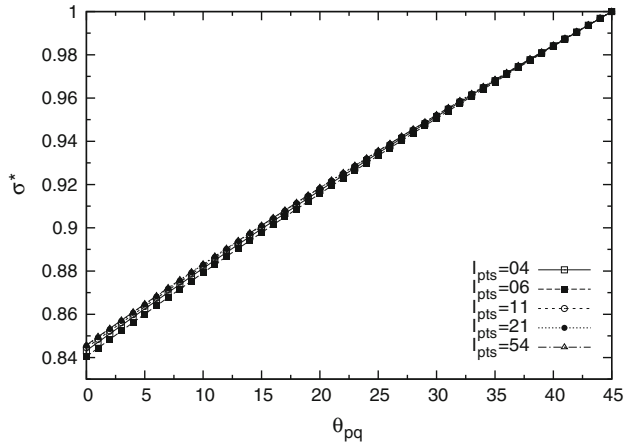

Fig. 7 Normalized grain boundary energy of a two-grain system as a function of the misorientation angle across the boundary for different number of interface points

directions. In Fig. 7 the GB energy is calculated for a 1D system with a flat interface between two grains and plotted against the misorientation, in degrees, between those grains. This is done following the procedure outlined by Cahn and Hilliard [27]. We normalize σ by its maximum value, σ^*. The values of the GB energy are for the case when there is no anisotropy due to the orientation of the plane GB, or the term γ^p_{ijkl} is zero. This procedure is then repeated with various numbers of points through the interface where the values reported on the legend of Fig. 7 correspond to the misorientation when $\theta_{pq} = 0$. As θ_{pq} increases so do the number of points through the interface. Thus the maximum error, when $\theta_{pq} = 0$ and $I_{pts} = 4$, is approximately 0.3%, when using $I_{\text{pts}} = 54$ as the appropriately resolved interface. This demonstrates that good accuracy of the GB energy is achievable in 1D with only four points through the interface. Furthermore, as the misorientation increases from zero and reaches 45° the GB energy changes by 15% in a linear manner.

Next 2D systems were employed to measure both the kinetics and morphology of a grain during its evolution from an initially circular grain. The two-grain system shown in Fig. 2a is used on a 512 × 512 grid along with a $\Delta t = 0.001$ due to the increased timestep restriction as a result of the fourth derivatives calculated in the evolution equation [18]. A value of μ was chosen ($\mu = 0.25$ which correlates to $I_{\text{pts}} = 11$ in the isotropic case) such that the number of the points through the interface would sufficiently resolve the kinetics based on the results from the previous sections. The effect of misorientation between grains is shown in Fig. 8 for when $\gamma_{\text{iso}} = -5$ and $\gamma_{\text{aniso}} = 15$. For low angle misorientations the two grains roughly favor the same interfaces (in this case the {11}) and therefore the middle grain appears faceted. However, at a misorientation of 45° one grain favors the {10} interfaces, whereas the other favors the {11}. The result is that the grain shape appears more isotropic as the misorientation approaches 45°. The reason for this occurs is because each gradient energy tensor is rotated to the computational frame of reference. Therefore when simulating a polycrystalline material in the limit where misorientation between grains is small, such as a textured material, the anisotropy will be clearly evident with the creation of triple point junction angles between grains such that the specified interfaces are favored. In the other limit, in a randomly oriented polycrystalline sample, the growth will more closely resemble that of an isotropic simulation, than in the previous case.

An advantage of this model is that the parameter γ_{aniso} can simply be increased or decreased to fine tune the amount of anisotropy desired for a particular system. In order to observe this effect we next keep the misorientation constant at 1° and the anisotropy parameters, γ_{aniso} and γ_{iso}, are varied as shown in Fig. 9. By examining Figs. 8 and 9 it is clear that values of $\gamma_{\text{aniso}} < 0$ have a minimum energy along the $\langle 10 \rangle$ and therefore favor {10} interfaces while values of $\gamma_{\text{aniso}} > 0$ are the reverse scenario and favor {11}

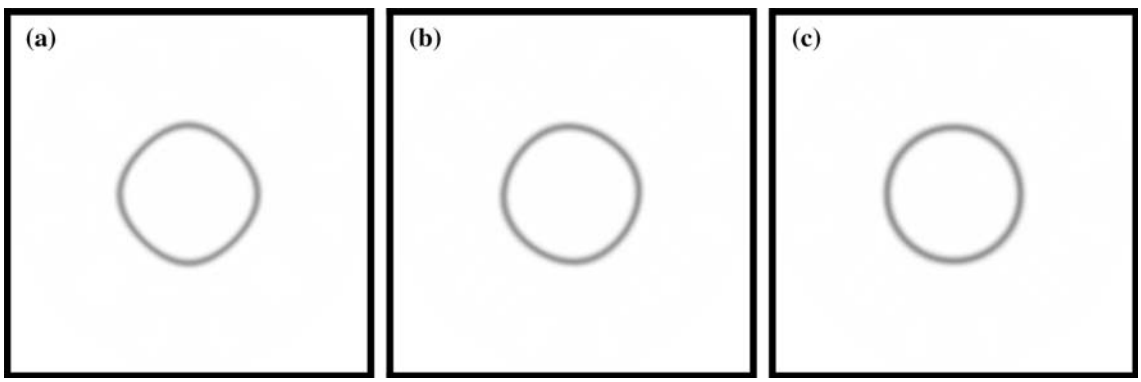

Fig. 8 Anisotropy parameters held constant at $\gamma_{\text{aniso}} = 15$, $\gamma_{\text{iso}} = -5$ while misorientation between the grains is set to **a** 1°, **b** 22.5°, and **c** 45°

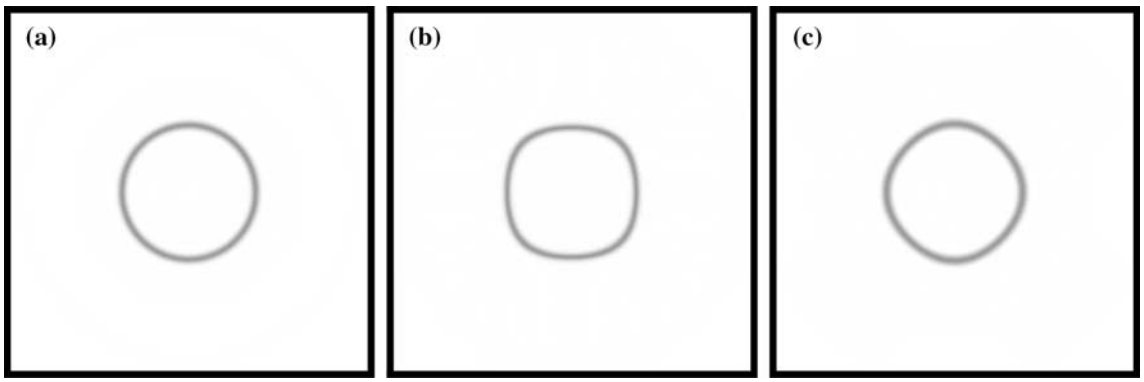

Fig. 9 Misorientation between grains is held constant at 1° while anisotropy parameters are set to **a** $\gamma_{aniso} = 0$, $\gamma_{iso} = 5$, **b** $\gamma_{aniso} = -15$, $\gamma_{iso} = 15$, and **c** $\gamma_{aniso} = 15$, $\gamma_{iso} = 5$

interfaces [15]. Since we measure the gradient energy tensor with respect to the crystallographic axes of each grain, a rotation of 45° of Fig. 9b is identical to Fig. 8a since the magnitude of γ_{aniso} is fixed. Furthermore, an additional comparison between Figs. 8a and 9c shows the amount of anisotropy, determined by γ_{aniso}, is roughly equivalent in both pictures. The values chosen in this article show a moderate amount of anisotropy but these can be modified such that sharp corners will develop [18].

Depending upon if one transverses along the $\langle 10 \rangle$ or the $\langle 11 \rangle$ the thickness of the interface and associated number of points through the interface will vary and will either be a minimum or maximum along those two directions. The ratio of the thickness along the two directions is dependent on the values chosen for γ_{aniso} and γ_{iso} in the two grain case. When there is more than one grain bordering another grain then the interface thickness is also dependent on the misorientation between the nearest neighbor grains. For the isotropic systems in the previous sections the interface thickness was constant and independent of direction. However, since this is no longer the case more care must be taken in picking an appropriate interfacial thickness used in determining the point at which deviation from the limit of dA/dt occurs when $R \gg T$. The interface thicknesses of all the anisotropic systems are calculated along the $\langle 10 \rangle$ and along the $\langle 11 \rangle$. Then the smaller of the two thicknesses is used to normalized the effective grain radius in order to be conservative in the measurement of the minimum R/T value for which a particular deviation from the model occurs. As in the case of the five-grain system, shown in Fig. 2b, we employ the same effective grain radius, $\sqrt{A/\pi}$, in all the simulations presented in this section. Then the growth rates of the various systems discussed previously are measured and plotted in Figs. 11 and 12. In Fig. 10 the anisotropy parameters are held at constant value of $\gamma_{iso} = -5$ and $\gamma_{aniso} = 15$ and the misorientation between the grains is varied from 1, 22.5, and 45°. In Fig. 11 the misorientation between the two grains is held constant at 1°

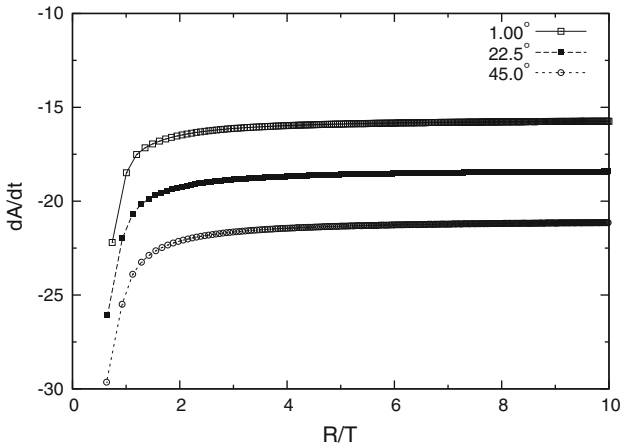

Fig. 10 dA/dt as a function of misorientation between grains in a two-grain system, where γ_{aniso} and γ_{iso} are held constant

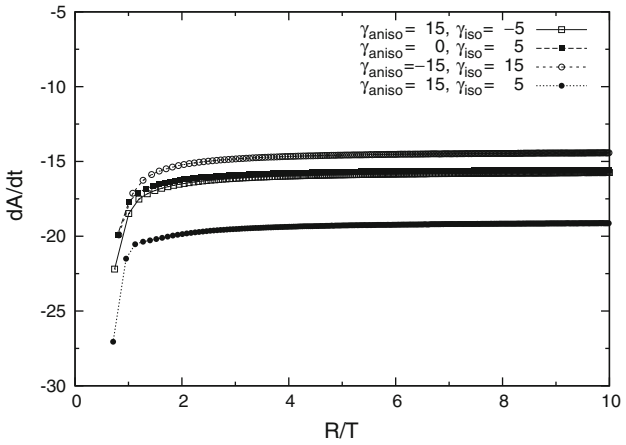

Fig. 11 dA/dt as a function of γ_{aniso} and γ_{iso} where misorientation between the grains, in a two-grain system, is held constant

and the anisotropy parameters are varied as shown in the legend of the figure. We report the un-normalized values of the growth rates of the grains due to the lack of sharp-interface results for this anisotropic model. Thus the curves

are not expected to converge on each other. The most obvious result is that the area of the grain decreases linearly with time when $R \gg T$. In all the 2D anisotropic systems presented in this section the same type of deviation behavior is clearly observable for when $R/T < 2$ as is for the isotropic systems, and slight deviations from a constant dA/dt are visible up to $R/T \approx 4$. From Fig. 10 we observe that when increasing the misorientation between the grains the shrinkage rate of the middle grain can be increased by up to 33%. Furthermore, comparison of dA/dt between these various systems in Fig. 11 yields the result that the shrinkage rate of the middle grain is faster the more positive the value of γ_{iso} or γ_{aniso}. Since the corresponding dA/dt curve of the middle grain decreased when $\gamma_{aniso} < 0$ the more negative the value of γ_{aniso} the slower the shrinkage rate, which is in agreement with the previous conclusions. This is because the grain boundary energy is higher for positive values of γ_{iso} and γ_{aniso}, resulting in a faster shrinkage rate, and grain shrinkage rate and boundary energy is lower when those terms are negative. Due to the different growth rate, dA/dt, of the grains the pictures shown in Figs. 8 and 9 are taken at different timesteps where the area of the center grains are equivalent.

The effect of these parameters on interface thickness are now investigated. When varying the misorientation between the grains from 1 to 45° the thickness of the interface increases by 5% along the ⟨10⟩ and increased by 23% along the ⟨11⟩, where the corresponding values of interface points increase from 13 to 14 along the ⟨10⟩ and from 8 to 10 along the ⟨11⟩. Next, we apply the same analysis for the effects of changing γ_{aniso} and γ_{iso} while holding the rotation constant at 1° between grains. Keeping $\gamma_{iso} = 5$ and changing γ_{aniso} from 0 to 15, the value of I_{pts} along ⟨10⟩ increases by 17%, a respective change of I_{pts} from 12 to 14. When $\gamma_{aniso} = 15$ and increasing γ_{iso} from −5 to 5 the value of I_{pts} changes from 13 to 14. Thus it appears that for a positive value of γ_{aniso}, or the more positive a value for γ_{iso}, the larger the number of interface points measured along the ⟨10⟩. Then when setting $\gamma_{aniso} = -15$ and $\gamma_{iso} = 15$ the number of interface points dropped to 11, and thus it can be concluded that the more negative the value of γ_{aniso} the lower the value of I_{pts} measured along the same direction. Through careful analysis of Figs. 8a and 9c, which both have the same value of γ_{aniso} but different values of γ_{iso}, it reveals different interfacial thicknesses. The interface thickness is greater in Fig. 9c, therefore one can conclude that both parameters, γ_{aniso} and γ_{iso}, together control the thickness of the interface.

We show that the method presented can be easily extended to three-dimensions by the following example simulation. In Fig. 12, we show the microstructure from a 3D model system. The simulations are carried out on a 200 × 200 × 200 grid, with three distinct grains (a portion of which—a cube of 140 × 140 × 140—is shown in the figures). Figure 12a–c shows the central grain at $t = 10$,

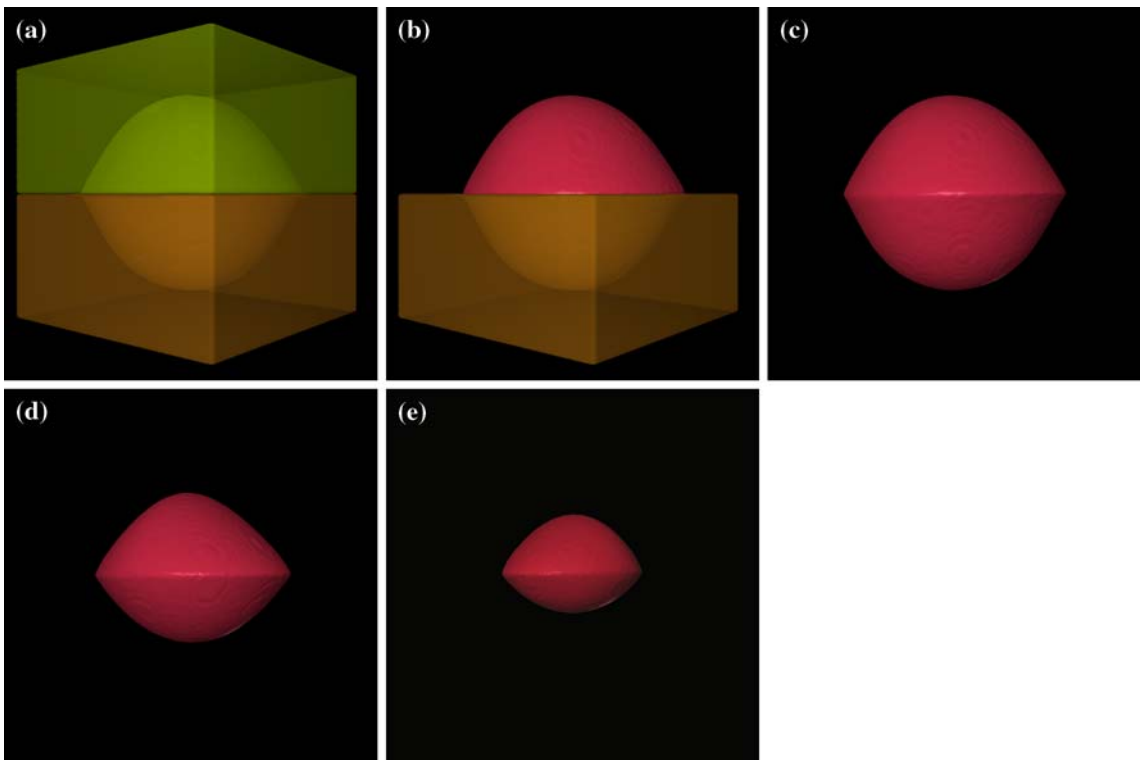

Fig. 12 Preliminary 3D results for an anisotropic three-order parameter system

with and without the top and bottom grains. Figure 12d shows the central grain at $t = 60$ and Fig. 12e shows the central grain at $t = 110$. The $\langle 100 \rangle$ directions of the central grain are oriented along the computational frame of reference, while the top capping layer is rotated by 1° and the bottom one by 45° about the z-axis.

For this 3D simulation, we have made the boundary energy dependent both on the misorientation across the boundary, and the planes of the grains that make up the boundary (anisotropy). More specifically, the boundary energy increases with increasing misorientation, and the anisotropy in the GB energies is such that the {111} boundaries are preferred compared with {100} boundaries. For the numerical values that we have used in these simulations, for a given misorientation, the boundaries made up of {111} planes have an energy that is smaller by 4% than boundaries made up of {100} planes. In addition, the upper boundary with a misorientation of 1° across has an energy that is smaller by nearly 6.5% than the lower boundary with a misorientation of 45°.

At the beginning of the simulation, at $t = 10$ for example (Fig. 12c) the central grain is near spherical, and is symmetric about the center; however, as the microstructure evolves, the grain shape becomes asymmetric. This asymmetry is determined both by the misorientation across the boundary and the anisotropy for any given misorientation. For example, in Fig. 12e, where the shape of the central grain at $t = 110$ is shown, the asymmetry in the shrinkage rate between the top and bottom parts of the grains is directly related to the misorientation across the two parts (1 and 45°, respectively, which translates to slower and faster shrinkage rates). In addition, for the top boundary, since both the grains prefer {111} or near {111} orientations, the boundary has noticeably lower mean curvature for orientations that are near {111}. On the other hand, at the bottom boundary, one grain prefers {111} and the other {100}; hence, the boundary structure that result is a compromise between the two, and in fact is more rounded. Thus, even in highly anisotropic systems that show faceted boundaries for small misorientations, the higher misorientation across a boundary can (and does) mask the anisotropy resulting in more smoother and rounded boundaries.

Conclusions

We have compared the results of 2D phase field simulations with both the von Neumann–Mullins result and Allen–Cahn sharp-interface asymptotics to identify the range of parameters for which the results from the phase field simulations converge to those of sharp interface calculations. We find that to obtain an agreement to within 10% with the sharp-interface and von Neumann–Mullins predictions of the kinetics of GB motion at least six mesh points through the interface are required along with interface thicknesses that are at least a factor of 2 smaller than the radius of curvature of the GB. When simulating large systems of grains, these criteria must be satisfied by the majority of the grains in the system. A model for grain growth has been developed that accounts for all five degrees of freedom of the grain boundary energy. It was observed that for a constant anisotropy in the GB energy, the larger the misorientation angle between grains the faster the shrinkage rate and thicker the grain boundary. Both the GB thickness and migration rate, through the variation in the anisotropic GB energy, were found to depend on the parameters characterizing the gradient energy tensor. Finally, preliminary results on 3D simulations have been presented in systems with both misorientation-dependent and anisotropic boundary energies indicating that both misorientation and anisotropy have a strong influence on the shapes of the growing/shrinking grains.

Acknowledgements We thank Yunzhi Wang and Dave Rowenhorst for useful discussions, and the Office of Naval Research (ONR-CNV0044048) for financial support.

References

1. Gottstein G, Shvindlerman LS (1999) Grain boundary migration in metals: thermodynamics, kinetics, application. CRC Press, New York
2. Sutton AP, Balluffi RW (1997) Interfaces in crystalline materials. Oxford University Press, Oxford
3. Humphreys FJ, Hatherly M (2004) Recrystallization and related annealing phenomena, 2nd edn. Elsevier, New York
4. Fionova LK, Artemyev AV (1993) Grain boundaries in metals and semiconductors. de physique edition, Les Ulis Cedex
5. Kang S-KL (2005) Sintering: densification, grain growth and microstructure. Elsevier, New York
6. Moelans N, Blanpain B, Wollants P (2008) Phys Rev B 78(024113):1
7. von Neumann J (1952) Metal interfaces. American Society of Metals, Cleveland, p 65. A written note to the paper of C. S. Smith
8. Mullins WW (1956) J Appl Phys 27:900
9. MacPherson RD, Srolovitz DJ (2007) Nature 446:1053
10. Thornton K, Agren J, Voorhees PW (2003) Acta Mater 51:5675
11. Chen L-Q (2002) Annu Rev Mater Res 32:113
12. Gururajan MP, McKenna IM, Voorhees PW (2008) Manuscript in preparation
13. Chen LQ, Yang W (1994) Phys Rev B 50:15752
14. Chen L-Q, Wang Y (1996) J Mater 48(12):13
15. Abinandanan TA, Haider F (2001) Philos Mag A 81(10):2457
16. Fan D, Geng C, Chen L-Q (1997) Acta Mater 45(3):1115
17. Fan D, Chen L-Q, Chen SP (1997) Mater Sci Eng A 238:78
18. McKenna IM, Gururajan MP, Voorhees PW (2008) Manuscript in preparation
19. Gruber J, Ma N, Wang Y, Rollett AD, Rohrer GS (2006) Model Simulat Mater Sci Eng 14:1189

20. Vedantam S, Patnaik BSV (2006) Phys Rev E 73:1
21. Kim SG, Kim DI, Kim WT, Park YB (2006) Phys Rev E 74(061605):1
22. Vanherpe L, Moelans N, Blanpain B, Vandewalle S (2007) Phys Rev E 76(056702):1
23. McKenna IM, Ma N, Gururajan MP, Wang Y, Voorhees PW (2008) Manuscript in preparation
24. Allen SM, Cahn JW (1979) Acta Metall 27:1085
25. Press WH, Teukolsky SA, Vetterling WT, Flannery BP (1992) Numerical recipes in Fortran, 2nd edn. Cambridge University Press, Cambridge
26. Fan D, Chen L-Q (1997) Philos Mag Lett 75(4):187
27. Cahn JW, Hilliard JE (1958) J Chem Phys 28(2):258